The Barents Sea frontal zones and water masses variability (1980–2011)

Laurent Oziel, Jérôme Sirven, Jean-Claude Gascard

Ocean Sci., 12, 169–184, 2016
www.ocean-sci.net/12/169/2016/
doi:10.5194/os-12-169-2016

Ocean Science Open Access EGU

The Barents Sea frontal zones and water masses variability (1980–2011)

L. Oziel, J. Sirven, and J.-C. Gascard

Sorbonne Universités (UPMC, Univ Paris 06)-CNRS-IRD-MNHN, LOCEAN Laboratory, IPSL, Université Pierre et Marie Curie, 75005, Paris, France

Correspondence to: L. Oziel (laurent.oziel@locean-ipsl.upmc.fr)

Received: 12 February 2015 – Published in Ocean Sci. Discuss.: 10 March 2015
Revised: 23 July 2015 – Accepted: 24 September 2015 – Published: 25 January 2016

Abstract. The polar front separates the warm and saline Atlantic Water entering the southern Barents Sea from the cold and fresh Arctic Water located in the north. These water masses can mix together (mainly in the center of the Barents Sea), be cooled by the atmosphere and receive salt because of brine release; these processes generate dense water in winter, which then cascades into the Arctic Ocean to form the *Arctic Intermediate Water*. To study the interannual variability and evolution of the frontal zones and the corresponding variations of the water masses, we have merged data from the International Council for the Exploration of the Sea and the Arctic and Antarctic Research Institute and have built a new database, which covers the 1980–2011 period. The summer data were interpolated on a regular grid. A *probability density function* is used to show that the polar front splits into two branches east of 32° E where the topographic constraint weakens. Two fronts can then be identified: the *Northern Front* is associated with strong salinity gradients and the *Southern Front* with temperature gradients. Both fronts enclose the denser Barents Sea Water. The interannual variability of the water masses is apparent in the observed data and is linked to that of the ice cover. The frontal zones variability is found by using data from a general circulation model. The link with the atmospheric variability, represented here by the Arctic Oscillation, is not clear. However, model results suggest that such a link could be validated if winter data were taken into account. A strong trend appears: the Atlantic Water (Arctic Water) occupies a larger (smaller) volume of the Barents Sea. This trend amplifies during the last decade and the model study suggests that this could be accompanied by a northwards displacement of the Southern Front in the eastern part of the Barents Sea. The results are less clear for the Northern Front. The observations show that the volume of the Barents Sea Water remains nearly unchanged, which suggests a northwards shift of the Northern Front to compensate for the northward shift of the Southern Front. Lastly, we noticed that the seasonal variability of the position of the front is small.

1 Introduction

1.1 The Barents Sea: a key region for water mass transformations

The Barents Sea (BS) extends over the northernmost Arctic shelf; it has a mean depth of about 230 m and covers about 1.4 million km^2 (Fig. 1a). The water mass distribution is strongly constrained by the cyclonic circulation, which dominates the BS (Fig. 1b), and the bottom topography, especially in the shallow areas. This circulation is forced by the Atlantic Water (AW) and the Norwegian Coastal Current Water, which flow into the BS through the Barents Sea Opening (BSO), an opening onto the shelf, which is 470 m deep at the deepest point. These eastward inflows amount to about 2 Sv (Ingvaldsen et al., 2002) and 1.1 Sv (Skagseth, 2008), respectively. Tides of high intensity are observed in the BS, principally in shallow and coastal areas (like the Svalbard or the Norwegian coast). They induce a significant turbulent mixing (Sundfjord et al., 2007).

The warm and saline Atlantic Water mixes in the BS with the fresh and cold Arctic Water (ArW) and with the Norwegian Coastal Current Water along the Norwegian coast (see Gascard et al., 2004; Fig. 1b). The BS thus plays a key role in the water masses transformation and is subject to large

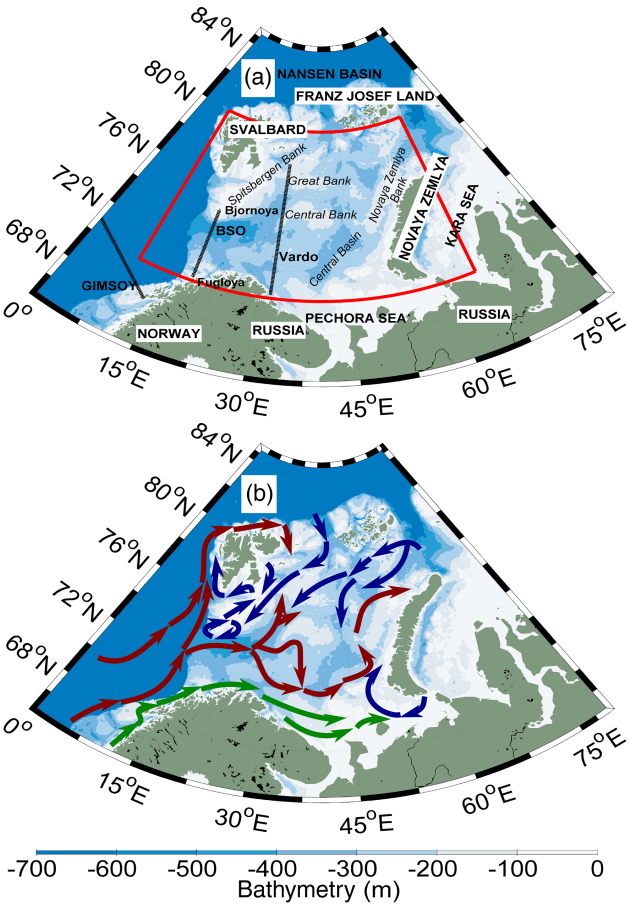

Figure 1. (a) Barents Sea map with bathymetry. The red line delimits the studied area. Repeated sections are represented in dashed black line: GIMSOY, BSO (Barents Sea Opening) and Vardø. **(b)** Schematic surface circulation of the main water masses (Atlantic Water: red arrows; Arctic Water: blue arrows; Norwegian Coastal Current: green arrows) (adapted from Harris et al., 1998).

hydrological contrasts. The salinity (S) is affected by the saline Atlantic Water, which is advected from the Norwegian Sea and the fresh water originating from the Norwegian Coastal Current Water (Baltic Sea), Arctic Water, rivers and ice melting; it can range from 33 to 35.2. The temperature also varies significantly, ranging from −1.8 °C for the Arctic Water (freezing point) to more than 10 °C for the Norwegian Coastal Current Water at the surface during summer.

The cooling and mixing of the Atlantic Water, Arctic Water and Norwegian Coastal Current Water, reinforced by brine rejections due to ice formation (especially around Svalbard, Franz Josef Land and Novaya Zemlya) and favorable conditions for shelf convection (Martin and Cavalieri, 1989), produce the dense Barents Sea Water (BSW). This Barents Sea Water mostly flows into the Arctic Ocean along the bottom between Novaya Zemlya (60° E/76° N) and Franz Josef Land (60° E/80° N) and partly contributes to the overturning circulation of the North Atlantic Ocean (Anderson et al., 1999). The Barents Sea Water also provides intermediate water to the Arctic Ocean at a depth of about 1200 m (Rudels et al., 1994; Schauer et al., 1997, 2002). All of these features and processes can be affected by climate change. Note that dense water is also produced in the Storfjord (Svalbard), but it flows to the west of Svalbard, into the Arctic Ocean through the Fram Strait. We do not consider this dense water source in this paper.

1.2 Climate change and low-frequency variability of the Barents Sea

During the past decade (1998–2008), the BS has experienced the largest reduction of sea ice cover in the Arctic (Screen and Simmonds, 2010) coupled with an air–ice–ocean system warming (Serreze et al., 2007). The annual sea ice extent has decreased by 50 %, reaching its lowest level (Årthun et al., 2012). The BS is becoming the first *ice-free* Arctic Sea (together with the Baffin Bay) in summer and autumn. In winter and spring, a seasonal marginal ice zone remains in the northern and sometimes eastern part of the BS, close to Novaya Zemlya. The north-eastern BS is the region where the sea ice variability is the largest (Inoue et al., 2012).

As the sea ice extent decreases, the region exposed to direct air–sea exchanges in the BS increases. The low-frequency variability of the Arctic is commonly associated with the North Atlantic Oscillation (NAO) or the Arctic Oscillation (AO) (Thompson and Wallace, 1998). Indeed, the AO and the NAO are highly correlated and both are useful for analyzing the impact of the atmospheric circulation on the Arctic. A negative (positive) AO generally corresponds to a cold (warm) atmospheric event over the eastern Arctic, a high (low) pressure anomaly and an anti-cyclonic (cyclonic) mode of the atmospheric circulation. Proshutinsky and Johnson (1997) showed that the AO affects the conditions along the western edge of the BS by modifying the Atlantic Water inflow through the BSO, between Fugloya and Bjornoya, and consequently the circulation in the BS. Indeed, a lower pressure over the Arctic (corresponding to a positive AO) strengthens the westerly winds in the inflow area and then increases the Atlantic Water penetration in the BS (Ingvaldsen, 2004). This would bring warmer Atlantic Water, decrease sea ice extent, enhance heat loss from the ocean to the atmosphere and increase meltwater content coming from the ice melting.

This simple scheme has been recently questioned. In a study limited to the 100–150 m layer of the Barents Sea, Levitus et al. (2009) also found that the multi-decadal variability was correlated with the Atlantic Multi-decadal Oscillation (AMO), which is an indicator of the temperature of the Atlantic Water and consequently of the Atlantic inflow. More recently, Seidov et al. (2015) analyzed the multi-decadal variability of the ocean north of 60° N and found that the waters were warming as a whole. However, they emphasized the fact that the average does not account for a very

complex situation, where some areas might even experience cooling episodes. They also found that multi-decadal variability of the ocean was more closely connected with the AMO than with the NAO, though the year to year changes of the AMO index were inversely correlated with those of the NAO (Yashayaev and Seidov, 2015). Note that the role of the AMO is not investigated in this paper since the AMO mainly helps to characterize the multi-decadal variability; the period we consider here is too short to allow such an analysis.

The role of the Atlantic Water in multi-decadal ocean variability has been analyzed in depth by Yashayaev and Seidov (2015) from the World Ocean Database. They found that the temperature records revealed a warming trend and a series of relatively warm and cold periods, which lag the periods of relatively low or high NAO events with a delay of about 4–5 years (the inverse for the AMO). They also showed that the Atlantic Water was transformed following two processes as it progressed northward. The evolution of salinity anomalies would be mainly due to the horizontal advection whereas the evolution of the temperature anomalies would be also controlled by the air–sea interactions. As a consequence of these two different processes, the temperature, salinity and density anomalies split and propagated separately in the Barents Sea.

Despite these recent progresses, the impact of the atmospheric interannual variability on the water mass transformations in the BS is still in debate. In winter, cold conditions favor ice production through latent heat exchanges between the ocean and the atmosphere releasing a large amount of salt, making the water denser. The production of Barents Sea Water would then be intensified. On the contrary, during warm conditions, sea ice formation is inhibited and consequently the open-ocean area is larger and well exposed to the atmospheric forcing, which facilitates the cooling of the ocean. It creates large sensible heat loss to the atmosphere, making also the water denser. This may still intensify the production of less dense Barents Sea Water.

1.3 Objectives

The BS plays an important role in the Northern Hemisphere climate (Smedsrud et al., 2013) by ventilating the Arctic Ocean with the dense Barents Sea Water (Aagaard and Woodgate, 2001; Schauer et al., 2002) and by being a place of high primary productivity (Loeng, 1991). The BS water masses delimited by several fronts are of particular interest. In this paper, we try to specify the mean state and variability for a 30-year period (1980–2011) of

1. The water mass distribution in a context of *Atlantification*. Arthun et al. (2012) defined this process as an increase of the heat transport from the Atlantic towards the BS due to an increase of the Atlantic Water transport and temperature and showed that it had occurred for at least the last decade. Johannessen et al. (2012) and Dalpadado et al. (2012) showed that the area covered by the Atlantic Water and the *mixed water* had slightly increased since 1970.

2. The fronts associated with the Atlantic Water, the Arctic Water and the Barents Sea Water. These fronts constitute a major oceanographic feature of the BS (Johannessen and Foster, 1978; Pfirman et al., 1994; Gawarkiewicz and Plueddemann, 1995), but have not been well studied. Only a few studies (e.g., Parson et al., 1996; Våge et al., 2014) provide local descriptions of the polar front, which separate the Atlantic Water from the Arctic Water in the western part of the Barents Sea. To our knowledge, no detailed description of the frontal structure has been done in the eastern part of the Barents Sea. Fronts are associated with some vertical mixing concomitant with vigorous ocean–air heat loss (~ 70 TW just for BS) of the Arctic (Serreze et al., 2007; Smedsrud et al., 2010), which favors the Barents Sea Water production in winter.

The BS is the only Arctic Sea with sufficient in situ observations to perform reliable analysis of the interannual variability in summer. We present in Sect. 2 the data we have gathered to produce a more comprehensive database than those previously used. A regional ocean circulation model (the SINMOD model; see Slagstad and McClimans, 2005) has also been used to complement the study of the variability. The following sections describe the mean position of the water masses and fronts and lastly their interannual variability and trend, which can be identified in the BS.

2 Data and methods

2.1 Data

The International Council for the Exploration of the Sea (ICES; http://ocean.ices.dk; see for example Nilsen et al., 2008) and the Arctic and Antarctic Research Institute (AARI; Russia, Ivanov et al., 1996; Korablev et al., 2007) provided processed hydrographic data sets that document the BS area. We have merged these data sets to form a new database, which parallels the "Climatological Atlas of the Nordic Seas and Northern North Atlantic" by Korablev et al. (2014). Both databases contain more than 130 000 temperature and salinity profiles; they include the BSO section repeated 6 times a year every other months, and the Vardø section repeated twice a year, in winter and summer (see Fig. 1a). They probably constitute the most complete hydrographic collection for the Barents Sea. By comparison, the World Ocean Database, discussed by Seidov et al. (2015), contains less than 85 000 profiles for an even larger area.

The techniques used to build these databases, however, slightly differ. Korablev et al. (2014) used the Data Interpolating Variational Analysis (DIVA) and thus obtained smoothed fields on a regular $0.25° \times 0.25°$ (latitude–

longitude) grid. This method has the advantage of taking into account topographic and dynamics constraints. We chose to use an unbiased kriging technique, which is described in the following subsection. The gridded fields are computed on a 0.5° × 0.25° grid. The fields we obtained are generally less smooth than those obtained by Korablev et al. (2014). They allow us to visualize the fields with more details, particularly around fronts. The data accuracy is difficult to specify. On rare occasions, the poorest accuracy might be 0.1 °C in temperature and 0.1 in salinity. However, after interpolation by kriging (see just below), the data associated with estimation errors below 20 % allowed us to build summer time series going from 1980 to 2011 for temperature and salinity.

2.2 Kriging: an optimal method for interpolating data

Kriging is an interpolation technique, which provides the best linear unbiased estimator of an unknown field (Journel and Huijbregts, 1978; Kitanidis, 1997). The originally sparsely sampled data are characterized by a semivariogram (or equivalently a covariance function), which depends only on the distance between measured sample points and represents their spatial correlation. This semivariogram is computed and then used to interpolate the data on a regular grid.

This technique first allowed us to derive temperature, salinity and density fields for each summer (August and September) from 1980 to 2011, on a grid whose resolution is 0.5°, × 0.25°. For each variable, four fields have been computed: the first field corresponds to the surface, the second field corresponds to an upper layer between 0 and 50 m (the high frequency variability is important in this layer and consequently the data are difficult to exploit), the third field corresponds to a mid-depth layer between 50 and 100 m (the vertical variations of the temperature and salinity are generally smaller than in the upper layer, and the low-frequency variability easy to detect) and the fourth field corresponds to a bottom, nearly homogeneous layer between 100 and 200 m. In order to have almost 100 % of the BS surface covered by the data set, the study area has been limited to the area shown in Fig. 1a (70–80° N 10–65° E). Data coverage is less dense on the eastern part of the domain (Fig. 2) because the observations became sparser in the Russian part of the BS during the last decade.

The same technique was used to interpolate the temperature and salinity fields from the Vardø section. The resolution of the (vertical) grid is 0.125° latitude × 5 m depth.

2.3 SINMOD 3-D model description and set-up (Slagstad, 1987)

SINMOD (SINtef Ocean MODel) is a coupled 3-D hydrodynamic chemical and biological model system that has been developed and used for more than 25 years at SINTEF (Scientist and Industrial Research Foundation, Norway). The hydrodynamic part of the model is based on the primitive equations, which are solved by finite differences using an Arakawa C grid (Mesinger and Arakawa, 1976). The model uses z coordinates in the vertical direction. The ice model is based on the elastic–viscous–plastic rheology (see Hunke and Dukowicz, 1997). The model is forced by transports through open boundaries (Slagstad and Wassmann, 1996), atmospheric fluxes provided by the European Centre for Medium-Range Weather Forecasts (ECMWF) reanalysis data (ERAi), freshwater input and tides. The four tidal components (M2, S2, K1 and N2) are imposed by specifying the transports at the open boundaries of the large-scale model. Data are taken from TPXO 6.2 (http://www.coas.oregonstate.edu/research/po/research/tide/index.html). Freshwater run-off, river discharge and run-off from land are based on outputs obtained from a simulation with a hydrological model (Dankers and Middelkoop, 2007). The model has been validated from in situ current measurements and temperature fields, and physical and chemical observations made at the Vardø section. More details about the model and its validation can be found in Slagstad et al. (1999) and Slagstad and McClimans (2005).

For this study, we used monthly temperature and salinity fields obtained from SINMOD runs performed for the 1979–2012 period over the whole Arctic with a 20 km grid resolution and 25 levels. Initial values of temperature and salinity were taken from the 1998 NODC World Ocean Atlas built by the NOAA-CIRES Climate Diagnostics Center, Boulder, Colorado, USA (http://www.cdc.noaa.gov/) to perform this experiment. For the 1997-2001 period, we also used a high-resolution (4 km and 34 levels) numerical experiment performed with the same model on a reduced domain covering the BS.

The low-resolution experiments are used to analyze the process leading to the observed variability of the temperature

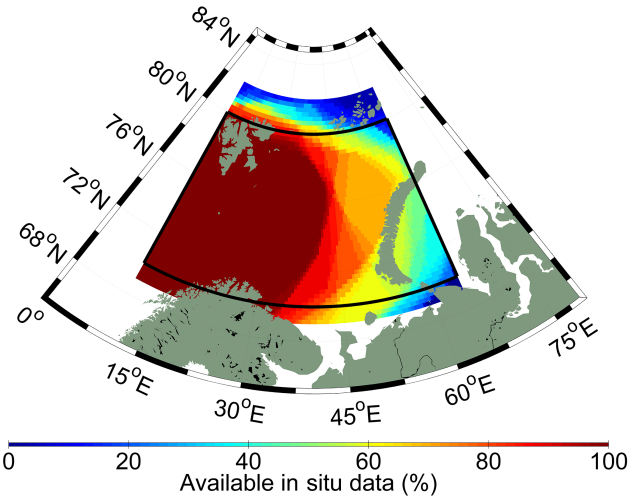

Figure 2. Available in situ data: percentage of data for the 1980–2011 period.

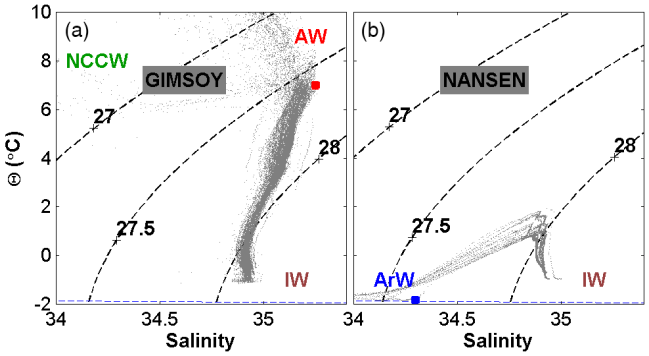

Figure 3. Potential temperature – salinity diagrams in August–September for the 1980–1985 period. **(a)** Gimsoy section **(b)** Nansen Basin. Red dot: ideal Atlantic Water; blue dot: ideal Arctic Water. Intermediate Arctic Waters: IW.

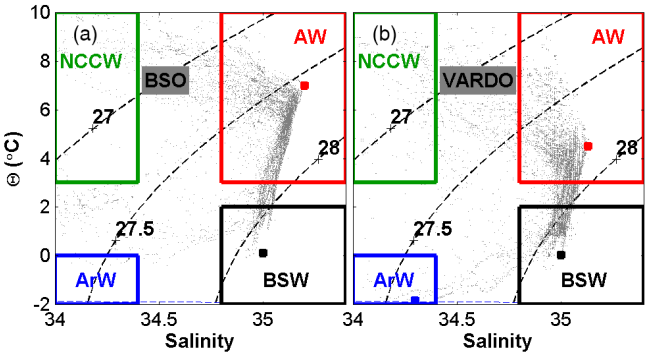

Figure 4. Potential temperature–salinity diagrams in August–September for the 1980–1985 period. **(a)** BSO section **(b)** Vardø section. Red dots: ideal Atlantic Water; black dots: ideal Barents Sea Water; and blue dots: ideal Arctic Water.

and salinity fields during the 1980–2011 period. The high-resolution experiment allowed us to study the changes experienced by the fronts between a cold and a warm period. In order to remove the *noise* due to the eddy activity, a Gaussian filter with a standard deviation of 36 km has been applied to the temperature and salinity fields.

3 Summer climatology of the water masses from the observations

3.1 Water masses

The analysis of the Θ–S diagram from repeated sections data enables us to characterize the water mass initial hydrological characteristics for the 1980–1985 period (Fig. 3). The water mass characteristics will be compared with the ones of the 2006–2011 period (see Sect. 4, Fig. 10) in order to characterize the amplitude of the hydrological changes, which occurred during the last 3 decades.

The Θ–S diagram of the Gimsoy transect in the Norwegian Sea (shown in Fig. 3a for the 1980–1985 period) enables us to identify the summer Atlantic Water (AW; depth $\sim$200 m, $T\sim7$ °C, $S\sim35.25$) and the summer Norwegian Coastal Current Water (NCCW; depth $\sim$50 m, $T>6$ °C, $S<34.4$), which both enter the BS. Note that the NCCW has a large seasonal variability in temperature and salinity: the temperature can reach more than 12 °C at the surface in summer and the salinity ranges from 32 to 34.4. The Intermediate Arctic Water ($T\sim-1$ °C, $S\sim34.9$) is found at a depth of around 1200 m and consequently cannot enter the BS.

North of 80° N, in the Nansen Basin, from surface down to about 100 m, the Arctic Water occurs, which can penetrate the BS. It can be clearly identified in the Θ–S diagram of Fig. 3b ($T<0$ °C, $S<34.7$).

Table 1. Water mass definitions for the Barents Sea.

Atlantic Water (AW):	$S>34.8$	$T>3$ °C
Arctic Water (ArW):	$S<34.7$	$T<0$ °C
Barents Sea Water (BSW):	$S>34.8$	$T\leq2$ °C ($\rho>1027.8$ kg m^{-3})
Norwegian Coastal Current : Water (NCCW)	$S<34.4$	$T>3$ °C
Meltwater (MW):	$S<34.4$	$0<T<3$ °C

The AW, NCCW and Arctic Water are thus found in the BS, with slightly modified characteristics. BSW and meltwater (MW) have a more local origin. Table 1 summarizes the characteristics of these five water masses for the BS; the given values are based on those generally found in literature. The square domains represented in the Θ–S diagrams in Fig. 4 have been built from these values.

These figures illustrate the large differences both in salinity and temperature of the water masses of the BS. The Barents Sea Water (also called *Barents Sea Atlantic derived water*, *modified Atlantic Water* or *Polar Front Water*) is formed on the BS shallow banks (central bank), mainly in winter, by the mixing of the other water masses and by large heat losses. For example, the temperature of the Atlantic Water is about 6 °C at BSO, which agrees with Årthun and Schrum (2010), whereas that of the Barents Sea Water is about 0 °C between Nova Zemlya and Franz Josef Land (Gammelsrød et al., 2009). The Barents Sea Water then cascades down to deeper regions (Årthun et al., 2011) and the largest part finally flows out of the BS toward the Arctic Ocean to form the Intermediate Arctic Water (Rudels et al., 1994). The Barents Sea Water has a high density, often greater than 1028 kg m^{-3}. The densest Barents Sea Water (not shown) is found east of the Vardø section, and has nearly the same hydrographic properties as the Intermediate Arctic Water found at around 1200 m depth, outside the BS (see Fig. 3).

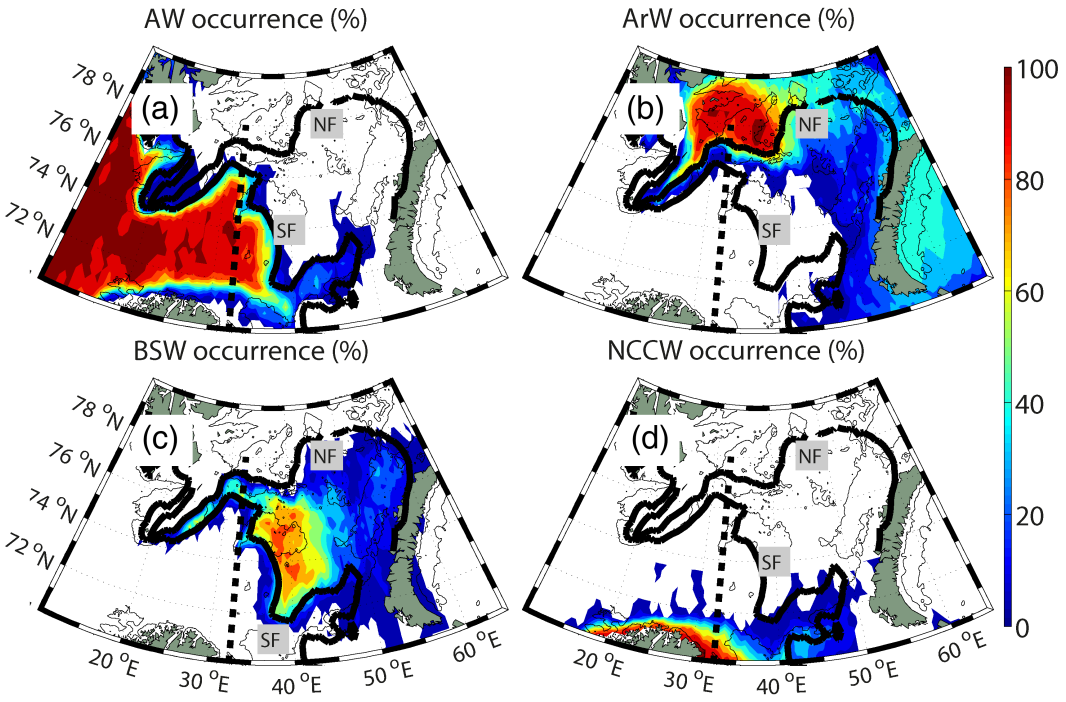

Figure 5. Water Mass Occurrences (%) over the 1980–2011 period in August–September for the 50–100 m layer. **(a)** Atlantic Water, **(b)** Arctic Water **(c)**, Barents Sea Water, **(d)** Norwegian Current Coastal Water. The *Southern Front* (SF) and *Northern Front* (NF) (bold black lines), the Vardø section (dashed line), and the 200 m isobath (thin black line) are indicated.

The Barents Sea Water scarcely appears in the BSO section (Fig. 4a) and becomes more visible in the Vardø section (Fig. 4b). This agrees with the results illustrated in Fig. 5, which characterizes the horizontal occurrence of water masses in August–September in the BS for the period 1980–2011. Only the layer between 50 and 100 m has been considered for this computation (see Sect. 2). A percentage of 100 % indicates that the water mass is present every summer in the concerned area. The Atlantic Water is always present in the south-west BS, the BSO trough and up to the Great Bank (Fig. 5a), and sometimes spreads further north and east in the deepest part of the BS such as the central basin (occurrence of about 20–30 % in these areas). The Arctic Water occurrence (Fig. 5b) is close to 100 % in the north-west BS and over the Spitzbergen bank. The locally formed Barents Sea Water (Fig. 5c) mainly resides over the central bank and in the central basin as expected (Årthun et al., 2011), but also in the eastern part of the BS. The Norwegian Coastal Current Water (Fig. 5d) has a significant contribution in the southern part of the BS accounting for about one-third of the inflowing waters through BSO. It remains near the coast, west of 30° E, then spreads up to 74° N with other waters from the White Sea, Pechora Sea, Kara Sea and rivers.

In the eastern part of the BS, the occurrence of a particular water mass is sometimes lower than 30 %, and no water mass is dominating east of 40° E. The shallow coastal area (depth shallower than 200 m) of the eastern BS is influenced by the four main water masses, i.e., the Atlantic Waters, Arctic Water, Barents Sea Water and Norwegian Coastal Current Water. This suggests that these different water masses can easily mix in this area. There is also a large contribution of ice in the fresh surface layer (not shown). Lastly, the dynamics of the BS is less constrained in the eastern part of the BS than in the western part due to smoother topography (Parson et al., 1996; Johannessen and Foster, 1978; Gawarkiewicz and Plueddemann, 1995). Consequently, the limits of the domains where the water masses are present no longer follow the isobaths.

3.2 Transformation of the water masses between BSO and Vardø

The temperature and salinity at the BSO and Vardø sections (Fig. 4) allow us to describe the transformations of the water masses moving across the BS in a more precise way. For this purpose, we define *ideal water masses*, which exemplify the specific properties of each water mass:

- Ideal Arctic Water (blue dots in Figs. 3b and 4b) is defined by a minimum of temperature since it is the coldest BS water mass.

- Ideal Barents Sea Water (black dots in Fig. 4) is defined by a maximum of density since it is the densest BS water mass.

– Ideal Atlantic Water (red dots in Figs. 3a and 4) is defined by a maximum of salinity since it is the most saline BS water mass.

An ideal Norwegian Coastal Current Water was not defined because the Θ–S points, which characterize it are too scattered. The characteristics of the Norwegian Coastal Current Water indeed depend on many external forcings (freshwaters inputs, solar heating, etc.).

As it progresses from Gimsoy to BSO, the ideal Atlantic Water experiences a weak decrease in salinity (of about 0.06) and a negligible decrease in temperature. The decrease in salinity is easily explained by mixing with the fresher Norwegian Coastal Current Water facilitated by the strong eddy activity (Gascard et al., 2004). The transformations are greater between BSO and Vardø: the salinity of the ideal Atlantic Water loses about 0.01 and the temperature more than 2 °C. They are caused by mixing with the adjacent Barents Sea Water and Arctic Water and chiefly by the strong sensible heat fluxes, which cool the surface water in winter, inducing a significant drop of the temperature of the Atlantic Water in the western part of the basin. Note, however, that the seasonal variations of the temperature and salinity remain small for the Atlantic Water and nearly vanishes for the Barents Sea Water along the Vardø section. We will show below (see Sect. 4) that the volume of Barents Sea Water on the contrary sustains considerable seasonal changes without involving important hydrological changes.

3.3 Fronts in the Barents Sea

The front that separates the Atlantic Water from the Arctic Water in the Barents Sea is denoted as the polar front. It follows the bottom topography in the western part and consequently remains stable from 1 year to the next. Its position is less clear in the eastern part and the new database presented in Sect. 2 can help clarify this. We thus computed the position of the fronts, which separate the Atlantic Water, the Arctic Water and also the Barents Sea Water. Indeed, the latter naturally appears when an objective interpolation method is employed.

The computation has been done for the summer data between 50 and 100 m (see Sect. 2), where the Atlantic Water is easily found. Below 100 m, the vertical mixing due to the turbulence generated by the tidal flow is strong (Parson et al., 1996) and the effects of salinity on the density compensate those of temperature. The existence of the fronts thus becomes more elusive because the density gradients vanish.

Fig. 6a and d show the mean temperature and salinity fields, respectively, obtained from the data described in Sect. 2 between 50 and 100 m (August–September of the 1980–2011 period). The temperature of the Atlantic Water in the south-western part of the basin exceeds 7 °C whereas that of the Arctic Water is below −1 °C in the north. The salinity ranges from less than 34 for the Norwegian Coastal Current Water close to the Norwegian coasts and for the Arctic Water in the northern part of the basin, and to more than 35 for the core of the Atlantic Water, which enters through the BSO. The temperature and salinity fronts are easy to distinguish in the western part of the basin in those figures, yet it is more difficult in the eastern part. Consequently, we have developed an algorithm, which allows one to determine the position of the fronts in a more objective way.

This algorithm is based on the computation of probability density functions (PDFs). We present it for the temperature field. First, the points where the temperature gradient exceeds $0.1\,^{\circ}\mathrm{C\,km^{-1}}$ are selected. The histogram of the temperature T of these points is built, representing the number of points for which this temperature is in the interval $T-\mathrm{d}T$ and $T+\mathrm{d}T$ with $\mathrm{d}T = 0.05\,^{\circ}\mathrm{C}$, where T represents the range of possible temperatures (see Fig. 6b). The PDF is obtained by dividing this number by the total number of points. The maximum of the PDF is determined, and the corresponding temperature of $Tm = 0.8\,^{\circ}\mathrm{C}$ is fixed. Finally, the standard deviation s is computed as $s = 2.4\,^{\circ}\mathrm{C}$. The frontal zone is defined by the area delimited by the isotherms $Tm - s/2 = -0.4\,^{\circ}\mathrm{C}$ and $Tm + s/2 = 2\,^{\circ}\mathrm{C}$. It is represented in Fig. 6a and c where the three isotherms (red lines) have been drawn. The area limited by the two extreme isotherms is the one where it is the most probable to find a temperature gradient exceeding the initial threshold $0.1\,^{\circ}\mathrm{C\,km^{-1}}$. The method is robust. The results do not significantly change when the threshold value for the gradient is slightly modified (for example when $0.10\,^{\circ}\mathrm{C\,km^{-1}}$ is replaced by $0.08\,^{\circ}\mathrm{C\,km^{-1}}$ or $0.12\,^{\circ}\mathrm{C\,km^{-1}}$).

The same method was used for the salinity, with a threshold value equal to $0.01\,\mathrm{km^{-1}}$, resulting in the PDF curve shown in Fig. 6e. The frontal area is then delimited by the isohalines $S = 34.45$ and $S = 34.75$ (mid-value: 34.6). It is represented in Fig. 6d and f where the three isohalines (blue lines) have been drawn.

In the western part of the BS, the frontal areas computed from the temperature or salinity fields are narrow, overlapping and associated with strong gradients (see Figs. 6 and 5), and follow the bottom topography as expected. The situation is more complicated east of the Vardø section. Two frontal areas clearly appear: a northern one associated with the salinity gradients (of about $0.004\,\mathrm{km^{-1}}$; see Fig. 6f), and a southern one associated with the temperature gradients (of about $0.05\,^{\circ}\mathrm{C\,km^{-1}}$; see Fig. 6c). To distinguish them, we denoted the first one the *Northern Front* and the second one the *Southern Front*. They are partly linked to the bottom topography: the Northern Front heads north, up to the 79° N latitude and the Southern Front heads south, crossing over the central bank, up to the central basin. Note that the 2 °C isotherm, which shows the southernmost position of the Southern Front (see Fig. 6c), is located further south than the front defined by Harris et al. (1998) in the eastern BS.

This description is compatible with the results of the previous subsection and those found in literature (see for example Parson et al., 1996 or Harris et al., 1998).

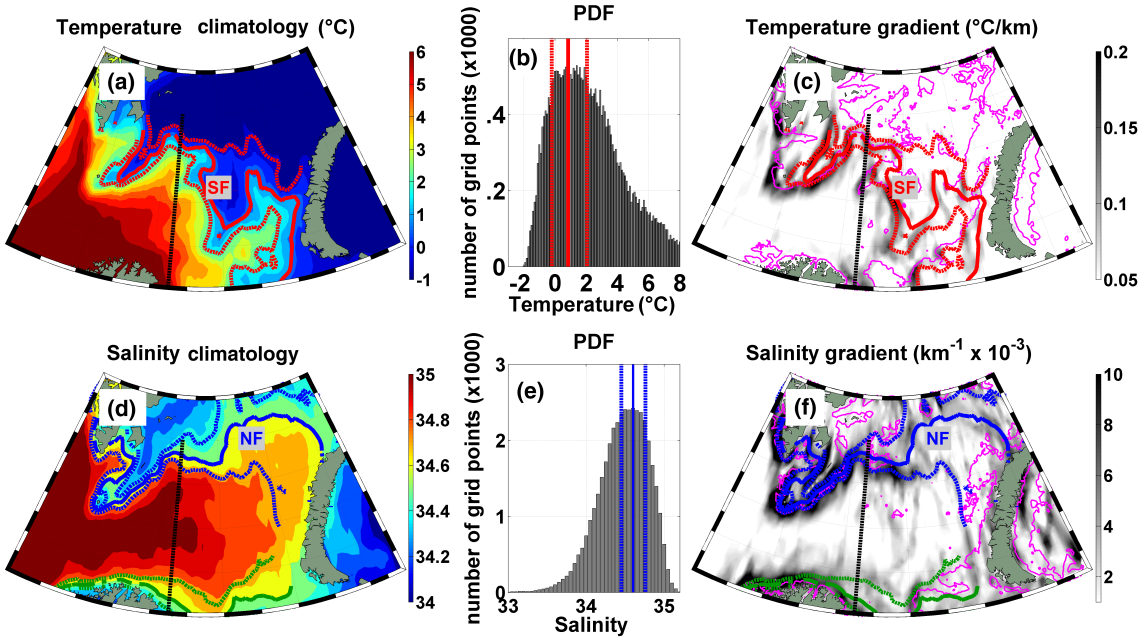

Figure 6. Temperature (°C) **(a)** and salinity **(d)** climatology for the 1980–2011 period (50–100 m layer, August–September). Probability density functions (PDFs) of the temperature and salinity fields are respectively shown in **(b)** and **(e)**. Horizontal gradients of temperature **(c)** and salinity **(f)**. The Southern Front (SF) (between the dashed red lines, +2 and −0.3 °C isotherms) and the Northern Front (NF) (between the dashed blue lines, 34.45 and 34.75 isohaline) are shown. Vardø section: black dashed line.

It is clear from Fig. 7 that the front at about 74° N is dominated by the temperature gradient. The situation is more complex for the other fronts. Consequently, to evaluate the impact of the temperature and salinity gradients on the density gradients, we have computed the dimensionless horizontal density ratio Dx defined by Rudnick and Ferrari (1999):

$$D_x = \alpha . T_x / \beta S_x,$$

where α is the thermal expansion coefficient of the seawater, β is the haline contraction coefficient, T_x and S_x are horizontal temperature and salinity gradients in $°C\,m^{-1}$ and m^{-1}, respectively, shown in Fig. 7c and d. The result of this computation is shown in Fig. 7e: the *Norwegian Coastal Current Front* and the Northern Front are dominated by the effects of salinity ($D_{x<1}$; blue) whereas the Southern Front is dominated by those of the temperature ($D_{x>1}$; red).

4 Variability of the Barents Sea Water masses

4.1 Environmental parameters variability

The AO (see Fig. 8a) index, is defined as the leading empirical orthogonal function of the wintertime sea-level pressure field, and according to Thompson and Wallace (1998) it was the dominant pattern of the atmospheric interannual and decadal variability over the Arctic. When this index is low, the atmospheric circulation becomes more anti-cyclonic and the air temperature decreases over the eastern Arctic. Consequently, the heat fluxes between the atmosphere and ocean are enhanced, particularly in winter. Furthermore, the westerlies are weakened and advect less Atlantic Waters into the BS from the Norwegian Sea through the BSO. The consequences of these changes are well marked in the BS. For example, the maximum extent of the sea ice (Fig. 8b, see also Furevik, 2001), which is a good indicator of the climate in the BS area (Serreze et al., 2007) is significantly correlated with the AO index (the correlation is about −0.33). As expected, a maximum of the sea ice extent is generally associated with a low AO index, as shown in Fig. 8 by the vertical blue bands enhancing the correlations. Similarly, the correlation between the winter (March) sea surface temperature (SST) or air temperature at 2 m (T2) in the BS (Fig. 8c) and the AO index, of about 0.36 and 0.23, respectively, is significant (both anti-correlations between the winter SST or T2 and the maximum extent of sea ice reach −0.55).

In addition, the BS has experienced remarkable climate changes for the past decades. For example, the maximum sea ice extent (Fig. 8b) has decreased by about 200 000 km^2 between 1980 and 2011, the T2 (Fig. 8c) has increased by about 2 °C and numerical modeling indicates that the ocean heat losses have been reduced by about $-50\,W\,m^{-2}$.

To detect the links between the interannual variability of the atmosphere and that of the water masses in the BS, a yearly index has been defined for each water mass, equal to the relative volume occupied by this water mass. This relative

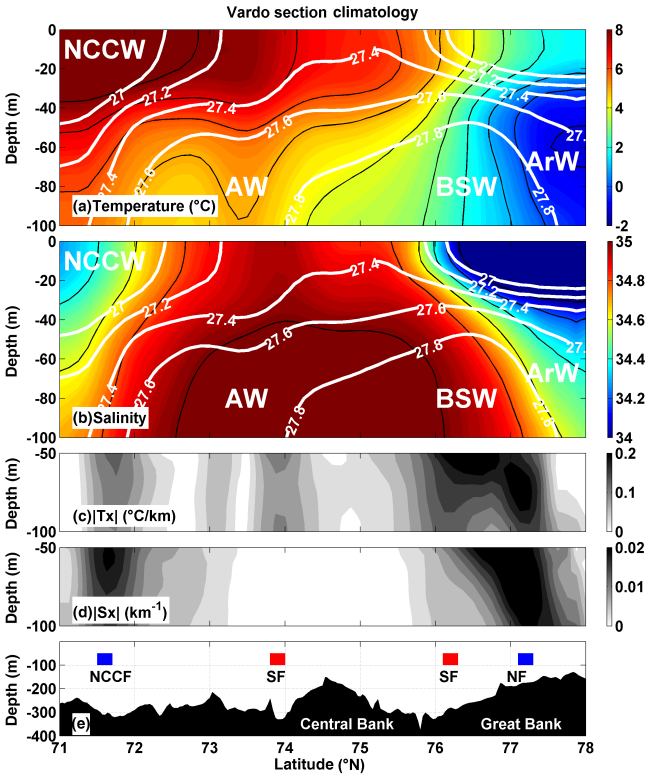

Figure 7. August–September climatology at Vardø section for the 1980–2011 period: temperature (°C) **(a)**, salinity **(b)**. White lines: isopycnals. Black lines: isotherms and isohalines (intervals: 1 °C and 0.1). Norms of horizontal temperature gradient **(c)** and salinity gradient **(d)**. Bathymetry **(e)**. The red and blue vertical patches respectively show which front is dominated by the temperature ($D_{x>1}$) or salinity ($D_{x<1}$) gradients.

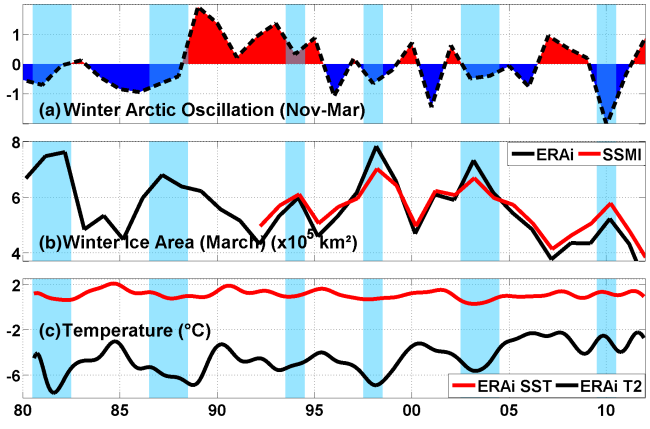

Figure 8. Interannual variations from 1980 to 2011 of (a) winter Arctic Oscillation (November–March) from NOAA. (b) Maximum sea ice extent (March). Black line: ERAi re-analysis, red line: from SSMI. (c) Low-passed (14 months) air temperature at 2 m and SST from ERAi re-analysis.

volume is obtained by adding the volumes of each grid cell

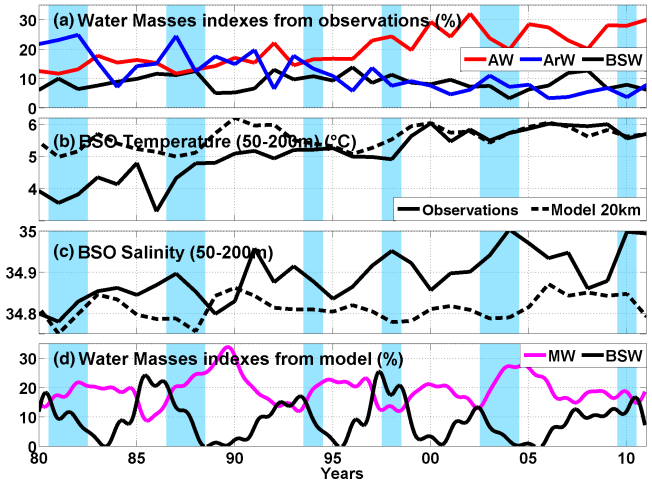

Figure 9. Interannual variations from 1980 to 2011 of **(a)** Atlantic Water in red (AW), Arctic Water in blue (ArW) and Barents Sea Water in black (BSW) index from in situ observations. **(b)** Temperature and **(c)** salinity (50–200 m) at BSO section from observations (solid line), SINMOD model (dashed line). **(d)** Barents Sea Water (BSW) and meltwater (MW) from the SINMOD model (a low-passed filter (14 months) has been applied).

where a water mass is present and dividing the sum by the total volume of all the grid cells. The computation based on the database of Sect. 2 has been done between 0 and 200 m depth. The corresponding series for the Atlantic Water, Arctic Water and Barents Sea Water indices are shown in Fig. 9a. The correlation between the AO index and the Atlantic Water or the Arctic Water index is not significant; however, the correlation between the Atlantic Water (resp. Arctic Water) and the winter ice cover reaches −0.30 (resp. 0.42) and is significant. Indeed, when the winter ice cover is low, the Atlantic Water index is generally high and the Arctic Water index low (for example in 1983–1984, 1990–1991, 2000, and 2007). The Atlantic Water and Arctic Water are strongly anti-correlated (correlation of about −0.75). The reverse occurs when the ice cover is high.

4.2 Water mass variability from observations study

The climate change observed in the atmosphere in the BS area is also obvious in the ocean data. The Atlantic Water index (resp. Arctic Water index) shown in Fig.9a presents a trend over the last 30 years, with perhaps an amplification during the last decade. The volume occupied by the Atlantic Water (Arctic Water) is about twice as large (as small) at the end of the series than at the beginning. On the contrary, no important trend can be detected on the Barents Sea Water index.

This is compatible with the recent sea ice loss caused by an Atlantification of the Barents Sea, due not only to an increase of the Atlantic Water temperature as described by Årthun et al. (2012), but also to the increase of the Atlantic Wa-

ter volume present in the BS. This is also compatible with the results of Johannessen et al. (2012) and Dalpadado et al. (2012), who identified an increase of the area covered by the Atlantic Water in the Barents Sea since 1970. However, our result differs from theirs. Indeed, the increase they found is much less important than the one we found. The methods used in their work are noticeably different, which could explain the differences between the results. They computed the area covered by the Atlantic Water by only considering the temperature between 50 and 200 m (against 0–200 m in our study) in the area 20–50° E and 72–80° N (against 10–60° E and 70–80° N) and they used a threshold value of 3 °C to define the Atlantic Water. Using the combined temperature-salinity signature to characterize the water masses, we were able, in this work, to distinguish between five water masses (Atlantic Water, Arctic Water, Barents Sea Water, Norwegian Coastal Current Water, meltwater). Our analysis is therefore probably more complete.

The processes leading to the Atlantification of the BS can be understood from the analysis of the Gimsoy, BSO and Vardø sections. The ideal Atlantic Water (see the definition in Sect.3) at the Gimsoy section (Fig. 10a) experiences an increase of about +1 °C in temperature and +0.05 in salinity during the last 30 years. An increase is also observed at BSO and Vardø sections with +0.2 °C/+0.05 (Fig. 10b) and +1 °C/+0.02 (Fig. 10c), respectively. These changes are represented by the red lines in Fig. 10. The changes at BSO are perhaps made more visible in solid line in Fig. 9b and c, which show the series of the mean temperature and salinity between 1980 and 2011. The mean has been computed from the database between 50 and 200 m. A trend of about +1 °C and +0.2 is found on these series. These values are compatible with those found at Gimsoy section for the ideal Atlantic Water. At the Vardø section, the temperature and salinity of the ideal Barents Sea Water remain nearly constant. The Θ–*S* diagram from the Nansen Basin is not shown because no changes have been detected in the Arctic waters.

These figures (Fig. 10) suggest that the hydrographic changes in the BS are driven by the inflow of Atlantic Water, which has become warmer in recent years. This warmer water, coming from the Norwegian Sea, invaded the BS and could prevent or slow down the formation of Barents Sea Water. This increase of Atlantic Water temperature is accompanied by an increase of Atlantic Water volume transport reported by Årthun et al. (2012).

The results based on the observations are mainly obtained from summer data, and thus ignore the hydrological conditions during the largest part of the year. This may be problematic since the volume of Barents Sea Water, being formed in winter, depends on winter conditions. Hence, using numerical models may help by complementing the information given by the observations and possibly reveal when and where observations are missing.

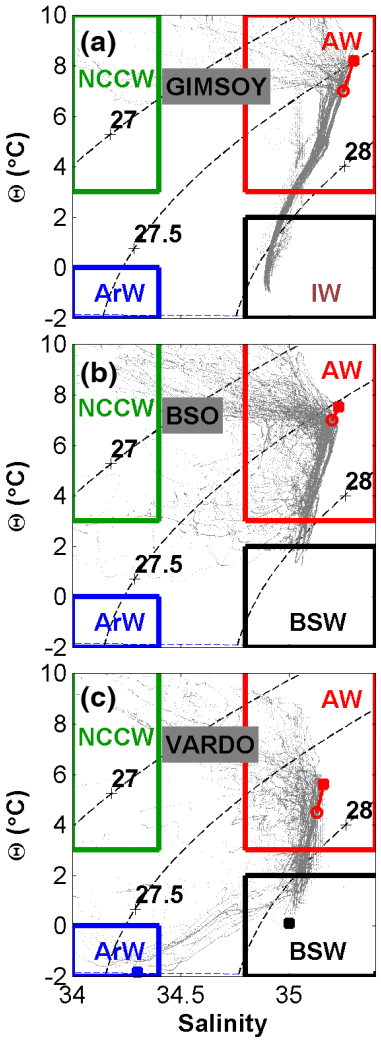

Figure 10. Potential temperature – salinity diagrams during the summer 2006–2011 period and shifts in the characteristics of the *ideal Atlantic Water* from the 1980–1985 period (empty circle) for **(a)** Gimsoy section, **(b)** BSO section and **(c)** Vardø section. Red dots: ideal Atlantic Water, black dot: ideal Barents Sea Water and blue dot: ideal Arctic Water. Intermediate Arctic Waters: IW.

4.3 Water mass variability from model study

The SINMOD model, which has been previously validated by its authors (see Sect. 2.3), is used in this section and the same methods are applied as with observations. The model, as any model (with a 20 km resolution), contains some biases: for example, it overestimates the temperature by about 1 °C for the first 12 years between 1980 and 1992 and underestimates salinity by about −0.1 (especially during recent years) along the BSO (dashed line in Fig. 9b and c). Similar biases are found along the other sections. More globally, the mixed layer is slightly too deep, the deep water is too homogeneous and the Barents Sea Water is slightly fresher and colder than the observations. However, the winter mech-

anism of the Barents Sea Water production is correctly represented (Fig. 9d) and the density is close to the observed density of the Barents Sea Water ($> 1027.8\,kg\,m^{-3}$). But the model is unable to reproduce the trend that we found in the observations for the BSO temperature and salinity (Fig. 9b and c). Such biases are not unusual for models and the causes of these flaws are numerous (see for example Sundfjord et al., 2007 or Ellingsen et al., 2009). Despite these imperfections, the model correctly reproduces the observed BS seasonal cycle (not shown) and succeeds in capturing the interannual variability.

To characterize the interannual variability, water mass indices have been computed for the SINMOD model, as it has been done for the observations. The correlation between the AO (Fig. 8a) and the Atlantic Water (Arctic Water) index of the model is equal to 0.42 (-0.23). The correlation between the ice cover and the Atlantic Water (Arctic Water) index of the model is also significant and equal to -0.42 (0.74). As for the observations, the Atlantic Water and Arctic Water index series are strongly anti-correlated (the correlation is about -0.50). These changes can be associated with the variations of the winter net heat flux over the BS; the correlation with the Atlantic Water index series reaches -0.46. This suggests that local mechanisms are important: the interannual changes observed in the Atlantic Water are not only due to remote changes, which could occur upstream, for example in the Norwegian Sea.

The model results, which take into account the temperature and salinity values in winter, partly agree with the results obtained from the summer observations, as the water mass variations in the BS are significantly correlated with the sea ice extent. However they differ concerning the AO. Significant correlations between the AO and the Atlantic Water or the Arctic Water indices are found in the model but not in the observations (though the ice extent is related to the principal mode of variability of the atmosphere over the Arctic). This discrepancy could be due to the fact that we only consider summer data in the analysis based on the observations.

At last, the model permits one to understand how well the Barents Sea Water (black line in Fig. 9d) is produced. The largest heat losses of the ocean occur when the differences between the winter air and sea surface temperature are maximum ($> 15\,°C$) and the ice cover is minimum ($500\,000\,km^2$). They can reach up to -200 or $-300\,W\,m^{-2}$. At that time the meltwater amount is generally maximum since the ice has melted and consequently the Barents Sea Water volume is small. Indeed, the water column is more stratified, the convection reduced and the Barents Sea Water formation inhibited. These conditions favor the formation of sea ice as illustrated in Fig. 8b (and can be viewed as a negative feedback). This induces the release of a large amount of salt, which in turn favors the formation of denser waters and consequently the Barents Sea Water formation. This mechanism is supported by the well-marked periodicity of the Barents Sea Water index time series (with a dominant period of about 5–6 years) and the large anti-correlation coefficients between the Barents Sea Water index time series and the heat loss (-0.65) or the meltwater amount (-0.82).

5 Variability of the fronts: a model study

The observations are too sparse – in particular in the eastern part of the BS – to study the variability of the fronts. Consequently, we used the high-resolution SINMOD model (see Sect. 2) to determine how a change in the climate conditions over the BS could affect the position of the Southern Front and Northern Front (see Sect. 3). To do this, the model has been integrated from 1998 to 2000.

In winter 1998, the AO index was negative and the ice covered more than $750\,000\,km^2$ of the BS. The mean air temperature was lower than $-6\,°C$. From 1998 to 2000, this situation has dramatically changed: the AO index became positive, the extent of the sea ice decreased by about $300\,000\,km^2$, the air temperature increased by about 6 °C, the mean SST by 0.5 °C and the mean temperature across BSO by 1 °C (Figs. 8 and 9b). Meanwhile, the volume occupied by the Atlantic Water increased (the Atlantic Water index increased from 25 to 30 %; Fig. 9a). The contrast between 1998 and 2000 therefore enables us to investigate how the Southern Front and Northern Front could shift if the climate keeps on warming and the Atlantification of the BS continues.

The high-resolution numerical model (4 km resolution) presents biases quite similar to the low-resolution one. The temperature (salinity) is about 1.5 °C (0.15) too high in comparison with the observations, the differences reaching 2.0 °C (0.25) in the eastern part of the basin. The model underestimates the mean volume of Atlantic Water but is able to represent its variability, as the Atlantic Water index increases by about 3 % (from 17 to 20 %), which seems acceptable, considering the short period of time (3 years) that is analyzed. The model also predicts a decrease of the Arctic Water index from 23 to 20 %, which seems compatible with the increase of Atlantic Water.

The technique used to compute the position of the fronts from the observations has been applied for the model results. The PDFs have been computed in summer and winter 1998 and 2000 for temperature (Fig. 11) and salinity (Fig. 12). The corresponding position of the fronts is shown in Fig. 13. The Northern Front is associated with the isohalines 34.7 in 1998 and 34.84 in 2000; the Southern Front is associated with the isotherms 1.4 °C in winter 1998, 3.4 °C in summer 1998, 1.9 °C in winter 2000 and 4.1 °C in summer 2000. The seasonal variability of the fronts (represented by the red and blue lines in Fig. 13) remains weak, even though the salinity gradients are more pronounced during winter: the former, associated with the Northern Front, increases from 0.04 to $0.055\,km^{-1}$. The temperature gradients are stronger in summer and the latter, associated with the southern part

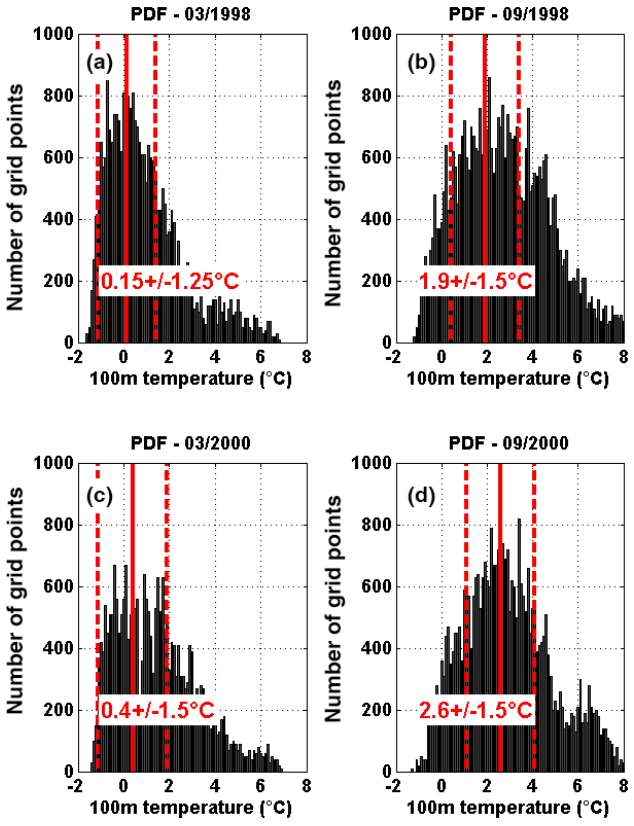

Figure 11. Probability density functions (PDFs) of the temperature fields (the period is indicated above each panel).

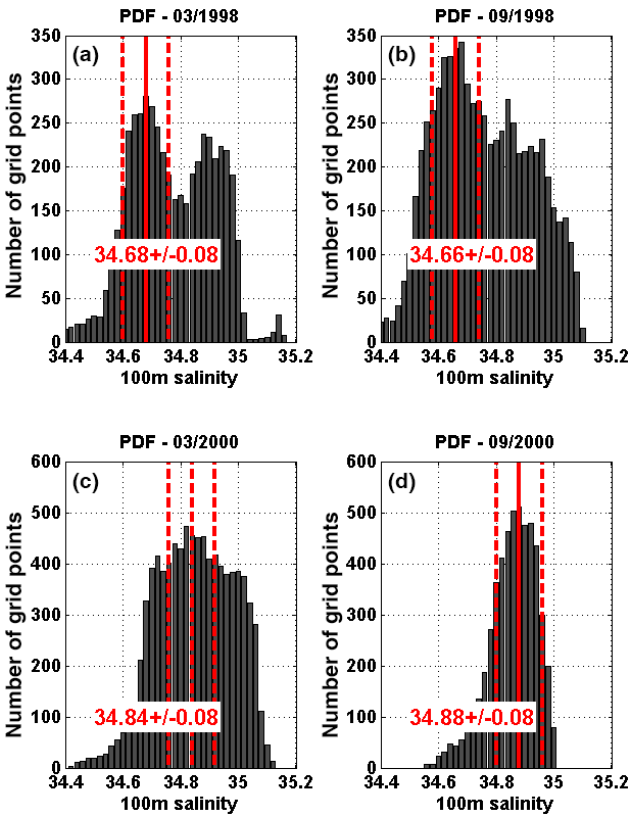

Figure 12. Probability density functions (PDFs) of the salinity fields (the period is indicated above each panel).

of the Southern Front, increase from 0.3 to 0.4 °C km^{-1} (not shown).

The interannual variability of the Northern Front is also negligible, though the climate conditions have changed. On the contrary, the position of the Southern Front is considerably modified, shifting eastwards and northwards, turning around the central basin, and following the 200 and 300 m isobaths. The temperature gradient then exceeds 0.06 °C km^{-1} around the Novaya Zemlya Bank. This shift obviously accompanies the increase of the Atlantic Water volume in 2000.

This high-resolution numerical experiment therefore suggests that the Atlantification of the BS observed during the last decade could induce a northward shift of the Southern Front. As the volume of the Barents Sea Water decreases from 20 to 25 % in 1998 to below 5 % in 2000, the position of Northern Front did not change.

Contrasting with this result, the observations suggest that the volume of the Barents Sea Water remained nearly unchanged from 1998 to 2000 (see Fig. 9a; no trend is found on the Barents Sea Water index). We thus can expect that the Northern Front shifts northwards to accompany the northwards shift of the Southern Front. The idealized character of the numerical experiment – which compares two states of the ocean over a short period – explains this difference.

6 Discussion and conclusions

The results presented in this study have been obtained from a new extensive hydrographic database, which is one of the most complete at the present time for this region. We built this database by merging the existing data sets with recent Russian data documenting the eastern BS.

Johannessen et al. (2012) and Dalpadado et al. (2012) showed that the area covered by the Atlantic Water and the *mixed water* had slightly increased since 1970. The new database revealed that this increase is more important than expected. Indeed we found that the Atlantic water volume had approximately doubled in 30 years. We associate this doubling to the Atlantification process suggested by Årthun et al. (2012) as an increase of the Atlantic inflow into the Barents Sea. A saltier and warmer inflowing Atlantic Water was observed from the Gimsoy section in the Norwegian Sea, up to the Vardø section in the central BS. Consequently, the domain occupied by the Atlantic Water extended further east and north. This especially affected the eastern BS at the expense of the Arctic Water that drastically decreased during

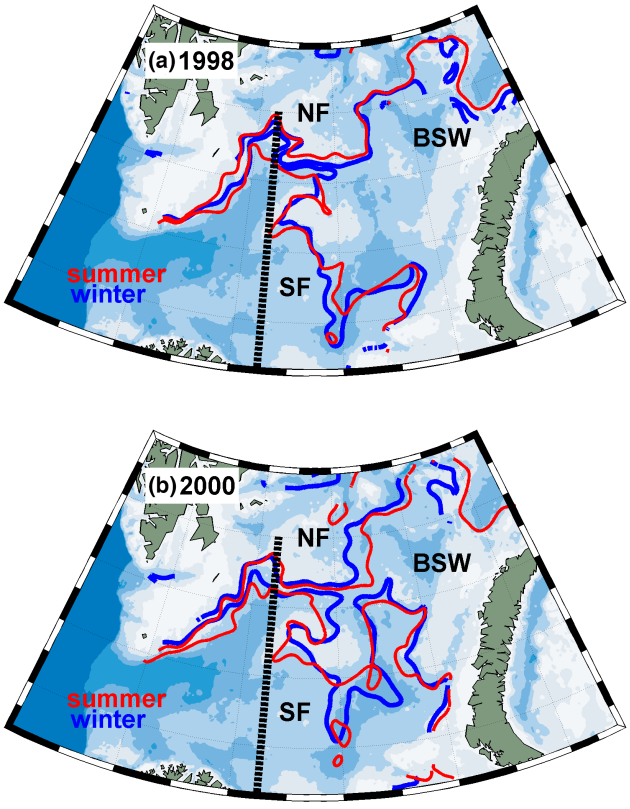

Figure 13. Seasonal and interannual variability of the Southern Front (SF) and Northern Front (NF). **(a)** 1998 and **(b)** 2000; (red line: summer; blue line: winter). The bathymetry and Vardø section are shown.

Glossary of acronyms	
AMO:	Atlantic Multi-decadal Oscillation
AO:	Arctic Oscillation index
AW:	Atlantic Water
ArW:	Arctic Water
BS:	Barents Sea
BSO:	Barents Sea Opening (BS AW entrance section)
BSW:	Barents Sea Water
MW:	Meltwater
NAO:	North Atlantic Oscillation
NCCF:	Norwegian Coastal Current Front
NCCW:	Norwegian Coastal Current Water
NF:	Northern Front
SF:	Southern Front

the last decade, as already observed by Lind et al. (2012). This trend was accompanied by a spectacular increase of the air temperature (Levitus et al., 2009). The last decade was the warmest of the last century (Boitsov et al., 2012) and is also characterized by the largest decrease of the sea ice extent in the BS ever observed (Parkinson and Cavalieri, 2012).

In the western part of the BS, the position of the polar front is constrained by the topography, following the Spitzbergen bank and the Great bank slopes. East of the Vardø section, the polar front splits into two branches, the so-called Southern Front and Northern Front. The Barents Sea Water is formed between these two fronts by mixing of the Atlantic Water with the Arctic Water and cooling. The eastern part of the BS is thus of first importance because it is the *mixing zone* where the dense Barents Sea Water formation takes place.

The interannual variability is also visible in the oceanic data. Cold (1981–1982, 1987–1988, 1994, 1998, 2003–2004 and 2010) and warm (1984, 1990–1992, 1995, 2000–1001 and 2007–2008) periods have been documented by Furevik et al. (2001) and Adlandsvik and Loeng (1991). Cold and warm events appeared clearly by looking at the variability of the sea ice extent, which is a good indicator of climate changes (Serreze et al., 2007). The sea ice extent variability was characterized by a period of about 5–7 years. We found that the variability of the Atlantic Water volume is significantly correlated with that of the sea ice extent: a maximum of the Atlantic Water volume generally corresponds to a minimum of the sea ice cover. The opposite is found for the Arctic Water. The causes of these variations are difficult to determine because of the complexity of the ocean–ice–atmosphere system in the BS; this complexity has been discussed (Karcher et al., 2003; Ingvaldsen et al., 2003; Dickson et al., 2000; Sando et al., 2010; Årthun et al., 2012). The variations of the Atlantic Water inflow into the BS, which show cycles with a period of about 7–10 years (Bengtssøn et al., 2004), could explain the variations of the Atlantic Water volume in the BS. The direct forcing by the atmosphere (westerlies) has an impact on the variability of the Atlantic Water inflow in the BS (Ingvaldsen et al., 2002). Finally, the occurrence of Arctic Water is clearly related to ice cover. More sea ice means more Arctic Water and vice versa.

The amount of observed data is sufficient only to extract pertinent scientific information only during summer. In consequence, the analysis of in situ observations has been done for August–September only. The use of the SINMOD model has enabled us to examine the winter situation. This was made possible because the model represents reasonably well the interannual variability. However, we found that the Atlantic Water and Arctic Water variability is significantly correlated with the AO index in the model, which contrasts with the observations. This might suggest that our data analysis based on the observations should be extended to winter data, even though the latter are scarce, to verify if this discrepancy persists.

Our results agree with Seidov et al. (2015) or Yashayaev and Seidov (2015). They emphasize the role of the AMO in comparison with that of the NAO. The AMO, which is a good indicator of the temperature of the Atlantic Water, is more directly linked to the Atlantic Water, which flows into the Barents Sea than the AO or the NAO. The corresponding indices

characterize global atmospheric changes and their local impact on the BS is more difficult to detect. Moreover, the AO, the AMO and the NAO are strongly correlated and a simple statistical analysis is not able to discriminate between their respective roles.

The variability of the fronts is not well constrained by the relatively few observations, which are particularly scarce in the eastern part of the BS, where the topographic guidance becomes small, allowing large displacements of the fronts. A study, with the high-resolution version of the SINMOD model, allowed us to compared the year 1998, during which the winter ice cover was large, with year 2000 in which it was small. We found that the Atlantic Water volume slightly increased (by about 3 %) and the Southern Front significantly shifted northward, while the Northern Front remained stationary. This suggests that the process of Atlantification could lead to a substantial northward displacement of the Southern Front. The Barents Sea Water would then move further north.

Aksenov et al. (2010) performed a high-resolution (1/12°) model study to determine the pathways of the North Atlantic Water into the Arctic Ocean. They found that the branch, which flows into the Barents Sea, shows complex circulation patterns. The bottom water they identified, lies in the south-eastern Barents Sea, close to the area where we observe the Barents Sea Water. Their model study allows them to elucidate the mechanisms that drive its formation, namely, full depth convection and mixing. The paths they identified for the Atlantic Water (the Franz Josef branch and the western part of the Novaya Zemlya Branch) are reminiscent of the frontal structures we describe in the eastern Barents Sea (The Northern Front and the Southern Front). Note that Karcher et al. (2003) had also suggested a similar pattern in a high-resolution model study.

The north-eastern part of the BS is one of the regions of the Arctic that is the most affected by the decline of the sea ice extent. As the sea ice is on the path of the Atlantic Water, it is suggested that the Atlantification of the BS could slow down the formation of sea ice in winter by bringing warmer water in larger quantities (higher Atlantic Water volume), and thus participate in the shrinking of the sea ice cover. This particularly endangers the sea ice of Novaya Zemlya Bank, which is crucial for the dense water formation in this area (Ivanov et al., 2005; note that a quite similar phenomenon had been observed north of Svalbard by Lind and Ingvaldsen, 2012). The formation of dense Barents Sea Water might stop then.

The BS can be considered as a robust *ocean cooler* and acts like a buffer zone between the World Ocean and the Arctic Ocean (Smedsrud et al., 2013). But at a time of drastic climate change, the ocean–atmosphere–ice system of the BS experiences important modifications. Our study suggests that the eastern part of the BS is the most affected region: Atlantic Water invades this area and has displaced the Southern Front northward. The long-term response to these changes on the dense water formation in the BS, and therefore on the Arctic ventilation, remains unknown. Finally, the BS accounting for 40 % of the primary productivity of the entire Arctic Ocean (Sakshaug, 2004), physical changes such as those described here could have a significant impact on the marine ecosystems of the BS.

Acknowledgements. The research leading to these results has received funding from the European Union under Grant Agreement no. 265863 within the Ocean of Tomorrow call of the European Commission Seventh Framework Programme. The EU project ACCESS funded the 3-year PhD of the lead author. The authors thank the two anonymous reviewers for their valuable comments and suggestions. The authors are particularly grateful to Michel Crépon for his many reviews. We also want to thank Xavier Capet for his help in the construction of the PDF method, and Michael Field for improvements on the final manuscript. The Hydrographic data were provided by the ICES Data Centre (www.ices.dk) and the Arctic and Antarctic Research Institute, Russia. The SINMOD model was provided by Dag Slagstad from SINTEF fisheries in Trondheim, Norway. The ERA-Interim data were obtained from the European Centre for Medium-Range Weather Forecasts data server. Arctic Oscillation data were down-loaded from JISAO, Seattle, USA. Ice concentration were obtained from SSMI satellite, NSIDC, USA.

Edited by: M. Hoppema

References

Aagaard, K. and Woodgate, R. A.: Some thoughts on the freezing and melting of sea ice and their effects on the ocean, Ocean Model., 3, 127–135, 2001.

Adlandsvik, B. and Loeng, H.: A study of the climatic system in the Barents Sea, Polar Res., 10 May 1990, 45–49, 1991.

Aksenov, Y., Bacon, S., Coward, A. C., and Nurser, A. J. G.: The North Atlantic inflow to the Arctic Ocean: High-resolution model study, J. Mar. Syst., 79, 1–22, 2010.

Anderson, L. G., Jones, E. P., and Rudels, B.: Ventilation of the Arctic Ocean estimated by a plume entrainment model constrained by CFCs, J. Geophys. Res., 104, 13423–13429, 1999.

Årthun, M. and C. Schrum: Ocean surface heat flux variability in the Barents Sea, J. Mar. Syst., 83, 88–98, 2010.

Årthun, M., Ingvaldsen, R. B., Smedsrud, L. H., and Schrum, C.: Dense water formation and circulation in the Barents Sea, Deep-Sea Res. Pt. I, 58, 801–817, 2011.

Årthun, M., T. Eldevik, Smedsrud, L. H., Skagseth, Ø., and Ingvaldsen, R. B.: Quantifying the influence of atlantic heat on Barents Sea variability and retreat, J. Climate, 25, 4736–4743, 2012.

Boitsov, V. D., Karsakov, A. L., and Trofimov, A. G.: Atlantic water temperature and climate in the Barents Sea, 2000–2009, ICES J. Mar. Sci., 69, 833–840, 2012.

Dalpadado, P., Ingvaldsen, R. B., Stige, L. C., Bogstad, B., Knutsen, T., Ottersen, G., and Ellertsen, B.: Climate effects on Barents Sea ecosystem dynamics, Ices J. Mar. Sci., 69, 1303–1316, 2012.

Dankers, R. and Middelkoop, H.: River discharge and freshwater runoff to the Barents Sea under present and future climate conditions, Clim. Change, 87, 131–153, 2007.

Dickson, R. R., Osborn, T. J., Hurrell, J. W., Meincke, J., Blindheim, J., Adlandsvik, B., Vinje, T., Alekseev, G., Maslowski, W., and Cattle, H.: The Arctic Ocean response to the north Atlantic oscillation, J. Climate, 13, 2671–2696, 2000.

Ellingsen, I., Slagstad, D., and Sundfjord, A.: Modification of water masses in the Barents Sea and its coupling to ice dynamics: a model study, Oc. Dynam., 59, 1095–1108, 2009.

Furevik, T.: Annual and interannual variability of Atlantic Water temperatures in the Norwegian and Barents Seas: 1980–199, Deep-Sea Res. I, 383–404, 2001.

Gammelsrød, T., Ø. Leikvin, Leikvin, Ø., Lien, V, Budgell, W. P., Loeng, H., and Maslowski, W.: Mass and heat transports in the NE Barents Sea: Observations and models, J. Mar. Syst., 75, 56–69, 2009.

Gascard, J., Raisbeck, G., Sequeira, S., Yiou, F., and Mork, K.A.: The Norwegian Atlantic Current in the Lofoten basin inferred from hydrological and tracer data (129I) and its interaction with the Norwegian Coastal Current, Geophys. Res. Lett., 31, L01308, doi:10.1029/2003GL018303, 2004.

Gawarkiewicz, G. G. and Plueddemann, A. J.: Topographic control of thermohaline frontal structure in the Barents Sea Polar Front on the south flank of Spitsbergen Bank, J. Geophys. Res., 100, 4509–4524, 1995.

Harris, C. L., Plueddemann, A. J., and Gawarkiewicz, G. G.: Water mass distribution and polar front structure in the western Barents Sea, J. Geophys. Res., 103, 2905–2917, 1998.

Hunke, E. C. and Dukowicz, J. K.: An elastic-viscous-plastic model for Sea Ice dynamics, J. Phys. Oceanogr., 27, 1849–1867, 1997.

Ingvaldsen, R., Loeng, H., and Asplin, L.: Variability in the Atlantic inflow to the Barents Sea based on a one-year time series from moored current meters, Cont. Shelf Res., 22, 505–519, 2002.

Ingvaldsen, R., Loeng, H., Ottersen, G., and Ådlandsvik, B.: Climate variability in the Barents Sea during the 20th century with focus on the 1990s, ICES J. Mar. Sci., 2019, 160–168, 2003.

Ingvaldsen, R. B.: Velocity field of the western entrance to the Barents Sea, J. Geophys. Res., 109, 1–12, 2004.

Inoue, J., Hori, M. E., and Takaya, K.: The role of Barents Sea Ice in the wintertime cyclone track and emergence of a warm-arctic cold-siberian anomaly, J. Climate, 25, 2561–2568, 2012.

Ivanov, V., Korablev, A., and Myakoshin, O.: PC-adapted oceanographic database for studying climate shaping ocean processes, Oceanology International 96, The Global Ocean-Towards Operational Oceanography, Conference proceedings, New Malden, UK, Spear-head Exhibitions Ltd, Vol. 1, 89–99, 1996.

Johannessen, O. M. and Foster, L. A.: A note on the topographically controlled Oceanic Polar Front in the Barents Sea, J. Geophys. Res., 83, 4567–4571, 1978.

Johannessen, E., Ingvaldsen, R. B., Bogstad, B., Dalpadado, P., Eriksen, E., Gjosaeter, H., Knutsen, T., Skern-Mauritzen, M., and Stiansen, J. E.: Changes in Barents Sea ecosystem state, 1970–2009: climate fluctuations, human impact, and trophic interactions, ICES J. Mar. Sci., 69, 880–889, 2012.

Journel, A. G. and Huijbregts, C.: Mining geostatistics, Academic press of San Diego University of California, ISBN 0123910501, 600 pp., 1978.

Karcher, M. , Kulakov, M. , Pivovarov, S. , Schauer, U. , Kauker, F., and Schlitzer, R.: Atlantic Water flow to the Kara Sea – comparing model results with observations, in: Siberian River Runoff in the Kara Sea: Characterisation, Quantification, Variability and Environmental Significance, edited by: Stein, F. and Fütterer, G., Elsevier, Proceedings in Marine Science, 47–69 , 2003.

Kitanidis, P. K.: Introduction to Geostatistics, Applications in Hydrogeology, Cambridge University Press, ISBN 0 521 58312 8, 1997.

Korablev, A., Pnyushkov, A., and Smirnov, A.: Compiling of the oceanographic database for climate monitoring in the Nordic Seas, in: Russian/Trudy AARI, 447, 85–108, 2007.

Korablev, A., Smirnov, A., and Baranova, O. K.: Climatological Atlas of the Nordic Seas and Northern North Atlantic, edited by: Seidov, D. and Parsons, A. R., NOAA Atlas NESDIS 77, 122 pp., doi:10.7289/V54B2Z78, 2014.

Levitus, S., Matishov, G., Seidov, D., and Smolyar, I.: Barents Sea multidecadal variability, Geophys. Res. Lett., 36, 1–5, 2009.

Lind, S. and Ingvaldsen, R. B.: Variability and impacts of Atlantic Water entering the Barents Sea from the north, Deep-Sea Res. Pt. I, 62, 70–88, 2012.

Loeng, H.: Features of the physical oceanographic conditions of the Barents Sea, in: Proceedings of the Pro Mare Symposium on Polar Marine Ecology, edited by: Sakshaug, E., Hopkins, C. C. E., and Britsland, N. A., Polar Res., 10, 5–18, 1991.

Martin, S. and Cavalieri, D. J.: Contributions of the Siberian shelf polynyas to the Arctic Ocean intermediate and deep water, J. Geophys. Res., 94, 12725–12738, 1989

Mesinger, F. and Arakawa, A.: Numerical methods used in atmospheric models, Global Atmospheric research programme – WMO-ICSU joint organizing committee, No. 17, 1, 1976.

Nilsen, J. E. Ø., Hátún, H., Mork, K. A., and Valdimarson, H.: The NISE dataset, Tech. Rep. 07-01, Faroes Fish. Lab., Tórshavn, Faroe Islands, 2008.

Parkinson, C. L. and Cavalieri, D. J.: Antarctic sea ice variability and trends, 1979–2010, The Cryosphere, 6, 871–880, doi:10.5194/tc-6-871-2012, 2012.

Parson, A. R., Bourke, R. H., Chiu, R. D. M. C., Lynch, J. F., Miller, J. H., and Plueddemann, A. J: The Barents Sea Polar Front in summer, J. Geophys. Res., 101, 14, 201–214, 1996.

Pfirman, S. L., Bauch, D., and Gammelsrød, T.: The Northern Barents Sea: Water Mass Distribution and Modification, Geophys. Monogr., 85, 77–94, 1994.

Proshutinsky, A. Y. and Johnson, M. A.: Two circulation regimes of the wind-driven Arctic Ocean, J. Geophys. Res., 102, 12493–12514, 1997.

Rudels, B., Jones, E. P., Anderson, L. G., and Kattner, G.: On the intermediate depth waters of the Arctic Ocean, Geophys. Monogr., 85, 33–46, 1994.

Rudnick, D. L. and Ferrari R.: Compensation of horizontal temperature and salinity gradients in the ocean mixed layer, Science, 283, 526–529, 1999.

Sakshaug, E.: Primary and secondary production in the Arctic seas, in: the Organic Carbon Cycle in the Arctic Ocean, edited by: Stein, R. and Macdonald, R. W., Springer, Berlin, 57–82, 2004.

Sandø, A. B., Nilsen, J. E. Ø., Gao, Y., and Lohmann, K.: Importance of heat transport and local air-sea heat fluxes for Barents Sea climate variability, J. Geophys. Res., 115, C07013, doi:10.1029/2009JC005884, 2010.

Schauer, U., Muench, R. D., Rudels, B., and Timokhov, L.: Impact of eastern Arctic shelf waters on the Nansen Basin intermediate layers, J. Geophys. Res., 102, 3371–3382, 1997.

Schauer, U., Loeng H., Rudels, B., Ozhigine, V. K., and Dieckf., W.: Atlantic Water flow through the Barents and Kara Seas, Deep-Sea Res. Pt. I, 2281–2298, 2002.

Screen, J. A. and Simmonds, I.: The central role of diminishing sea ice in recent Arctic temperature amplification, Nature, 464, 1334–1337, 2010.

Seidov, D., Antonov, J. I., Arzayus, K. M., Baranova, O. K., Biddle, M., Boyer, T. P., Johnson, D. R., Mishonov, A. V., Paver, C., and Zweng, M. M.: Oceanography north of 60° N from World Ocean Database, Prog. Oceanogr., 132, 153–173, 2014.

Serreze, M. C., Holland, M. M., and Stroeve, J.: Perspectives on the Arctic's shrinking Sea-Ice cover, Science, 315, 1533–1536, 2007.

Skagseth, Ø.: Recirculation of Atlantic Water in the western Barents Sea, Geophys. Res. Lett., 35, L11606, doi:10.1029/2008GL033785, 2008.

Slagstad, D. and McClimans, T. A.: Modeling the ecosystem dynamics of the Barents sea including the marginal ice zone: I. Physical and chemical oceanography, J. Mar. Syst., 58, 1–18, 2005.

Slagstad, D. and Wassmann, P.: Climate Change and carbon flux in the Barents Sea: 3-D simulations of ice-distribution, primary production and vertical export of particulate organic carbon, Mem. Natl. Inst. Polar Res., 51, 119–141, 1996.

Slagstad, D., Downing K., Carlotti, F., and Hirche, H. J.: Modelling the carbon export and air-sea flux of CO2 in the Greenland Sea, Deep-Sea Res. Pt. II, 46, 1511–1530, 1999.

Smedsrud, L. H., Ingvaldsen, R., Nilsen, J. E. Ø., and Skagseth, Ø.: Heat in the Barents Sea: transport, storage, and surface fluxes, Ocean Sci., 6, 219–234, doi:10.5194/os-6-219-2010, 2010.

Smedsrud, L. H., Esau I., Ingvaldsen, R. B, Eldevik, T., Haugan, P. M., Li, C., Lien, V. S., Olsen, A., Omar, A. M., Otterå, O. H., Risebrobakken, B., Sandø, A. B., Semenov, V. A., and Sorokina, S. A: The Role of the Barents Sea in the Arctic Climate System, Rev. Geophys., 51, 415–449, 2013.

Sundfjord, A., Fer, I., Kasajima, Y., and Svendsen, H.: Observations of turbulent mixing and hydrography in the marginal ice zone of the Barents Sea, J. Geophys. Res., 112, C05008, doi:10.1029/2006jc003524, 2007.

Thompson, D. W. J. and Wallace, J. M.: The Arctic oscillation signature in the wintertime geopotential height and temperature fields, Geophys. Res. Lett., 25, 1297–1300, 1998.

Våge, S., Basedow, S. L., Tande, K. S., and Zhou, M.. Physical structure of the Barents Sea Polar Front near Storbanken in August 2007, J. Mar. Syst., 130, 256–262, 2014.

Yashayaev, I. and Seidov, D.. The role of the Atlantic Water in multidecadal ocean variability in the Nordic and Barents Seas, Prog. Oceanogr., 132, 68–127, 2015.